

Interference of Mode Instabilities and Pattern Formation in Anharmonic Lattices

Victor M. Burlakov

Institute of Spectroscopy Russian Academy of Sciences, 142092 Troitsk, Moscow region, Russia

(Received 28 October 1997)

On an example of optically excited Klein-Gordon lattice, a striking new feature of anharmonic lattices related to dynamical coherent structure (pattern) formation is reported. It is shown that two factors are important for pattern formation: (i) lattice discreteness, which strongly reduces the number of lattice spatial modes among which the energy of external field is shared, and (ii) destructive interference of modulation instabilities of these modes resulting in stability of the pattern. Possible experimental realization is discussed. [S0031-9007(98)05985-7]

PACS numbers: 63.20.Ry

Dynamics of anharmonic lattices have been extensively studied in relation to energy sharing between lattice modes and recurrence phenomena [1–7], properties of intrinsic localized modes (ILMs) [4,8–13], and modulation instability (MI) of running and standing waves [14–20]. In the present Letter a striking new feature of periodically driven anharmonic lattices is described: coherent dynamical structure (pattern) formation resulting from MI of excited lattice spatial mode (LSM). So far patterns have been studied basically in continuous systems (see Ref. [21], and references therein) and recently in granular materials [22–25]. Some localized structures (one may call them “simplest patterns”) have also been found in driven lattices: kinklike structures were observed in the damped and parametrically driven lattice of coupled pendulums [26] and analyzed theoretically in the Klein-Gordon (KG) lattice [27]; ILM-like structures were described in both KG [28] and Fermi-Pasta-Ulam (FPU) lattices [29].

On an example of optically driven KG lattice with quartic anharmonicity, I show that the MI mediated pattern is actually formed by a small (3–5) number of LSMs, and its stability results from destructive interference of MIs of these LSMs. The interference effect in the MI is possible because of one and the same frequency of viscous vibration for all LSMs. It turned out that the stable pattern does exist in a rather broad region of the system and the driving force parameters. The analytical results are verified by numerical experiment, where the patterns have been found also in the quasi-two-dimensional KG and FPU lattices.

MI of the carrier LSM in the optically driven KG lattice.—Motion equation for n th particle of unity mass and charge in the KG lattice is

$$\partial^2 U_n / \partial t^2 + \gamma \partial U_n / \partial t + \omega_0^2 U_n + K_2(2U_n - U_{n-1} - U_{n+1}) + K_4 U_n^3 = E_0 e^{i\omega t} + \text{c.c.}, \quad (1)$$

where γ is a phenomenological damping constant, ω_0^2 , K_4 are in site, K_2 is intersite force constants, and E_0 is the external field amplitude. The solution of Eq. (1) for small anharmonicity can be found within the rotating wave approximation (RWA)

$$U_n(t) = \frac{1}{2} [V_C \exp(i\omega t + i\varphi) + \text{c.c.}], \quad (2)$$

where V_C and φ are real amplitude and phase angle, respectively. For $\omega < \omega_0$ the dependence $V_C \propto E_0$ shown in Fig. 1(a) reveals bistability and can be subdivided into

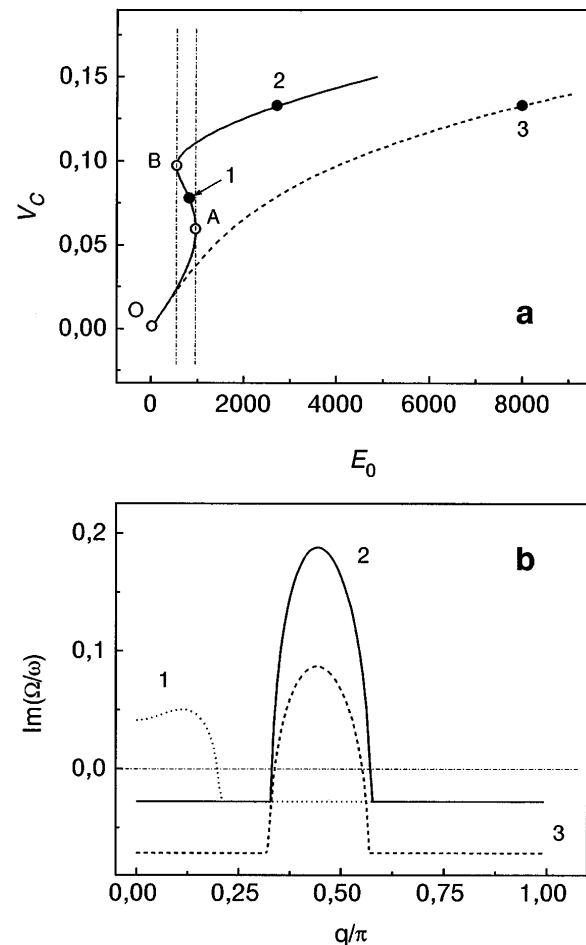


FIG. 1. (a) $V_C \propto E_0$ plot for $\omega = 0.9\omega_0$, $\gamma = 0.05\omega_0$ (solid line), $\omega = 1.05\omega_0$, and $\gamma = 0.15\omega_0$ (dashed line); symbols mark the numbered points at which (b) the calculated relative increment $\text{Im}[\Omega(q)/\omega]$ for a perturbation LSM is shown. Here, and for other figures, $\omega_0 = 200\sqrt{\pi}$, $K_2 = 6 \times 10^4$, and $K_4 = -\frac{8}{3}\pi^2\omega_0^2$.

three regions: OA , AB , and B^∞ , while for $\omega > \omega_0$ this dependence is monotonous. To study MI of the solution (2) we add the perturbation

$$\delta U_n = \frac{1}{2} \cos(qn) [V_{P1} \exp[i(\omega - \Omega)t] + V_{P2} \exp[i(-\omega - \Omega)t] + \text{c.c.}], \quad (3)$$

where V_{Pj} is the complex amplitude, and q and Ω are the wave vector and the complex frequency of the perturbation wave, respectively. The latter can be determined from the equation, obtained after substitution of (2) with perturbation (3) into Eq. (1)

$$\begin{aligned} [\omega_k^2 - (\omega + \Omega)^2 - i\gamma(\omega + \Omega)] \times \\ [\omega_k^2 - (\omega - \Omega)^2 + i\gamma(\omega - \Omega)] = \left(\frac{3}{4} K_4 V_C^2\right)^2, \end{aligned} \quad (4)$$

where $\omega_k^2 = \omega_0^2 + 4K_2 \sin(q/2)^2 + \frac{3}{2} K_4 V_C^2$. Relative increment $\text{Im}[\Omega(q)/\omega]$ is plotted in Fig. 1(b) for the ω and V_C values corresponding to the numbered points in Fig. 1(a). In the region OA of the $\omega = 0.9\omega_0$ curve in Fig. 1(a) $\text{Im}[\Omega(q)] = -\gamma/2$, i.e., the carrier LSM is stable. In the AB and B^∞ regions the carrier LSM possesses MI ($\text{Im}[\Omega(q \neq 0)/\omega] > 0$), besides the unstable amplitude value ($\text{Im}[\Omega(0)/\omega] > 0$) in the first region (curves 1 and 2 in Fig. 1(b), respectively). For $\omega = 1.05\omega_0$ the carrier LSM possesses MI at any E_0 value [curve 3 in Fig. 1(b)].

Pattern solutions.—At $t = 0$ there is a seeding LSM $\sim \cos(qn)$ in the lattice. Under action of the external field $E = E_0 e^{i\omega t}$, the system will pass through two stages: (a) excitation of $k = 0$ carrier LSM; (b) growing up of the seeding LSM due to MI of the carrier LSM and generation of other LSMs due to four-wave mixing. We restrict our consideration by the total number of the LSMs $N_{\text{LSM}} = 3$: with wave vectors $k_1 = 0$, $k_2 = \pi/2$, and $k_3 = \pi$ (lattice constant $a = 1$). Because of the symmetry arguments only standing waves (LSMs) are considered. No new LSMs important within RWA will appear due to four-wave mixing of the three chosen. Thus, the MI of the $k = 0$ carrier LSM must have a maximum around $q_{\text{max}} = \pi/2$. This is the condition for E_0 or, in other words, for the carrier LSM amplitude V_C . Note that V_C strongly increases with increasing q_{max} , therefore, the case of $N_{\text{LSM}} = 2$ ($q_{\text{max}} = \pi$) drops out of the RWA. The trial solution for the pattern in our case is

$$\begin{aligned} \delta U_n = \frac{1}{2} (\exp[i(\omega - \Omega)t] \{V_{P1} \cos(qn) + V_{P3} \cos[(\frac{\pi}{2} - q)n] + V_{P5} \cos[(\frac{\pi}{2} + q)n] + V_{P7} \cos[(\pi - q)n]\} \\ + \exp[i(-\omega - \Omega)t] \{V_{P2} \cos(qn) + V_{P4} \cos[(\frac{\pi}{2} - q)n] + V_{P6} \cos[(\frac{\pi}{2} + q)n] + V_{P8} \cos[(\pi - q)n]\} + \text{c.c.}) \end{aligned} \quad (6)$$

fulfills this condition. Indeed, all the aforementioned products result in a set of spatial harmonics with wave vectors $k_p = \pm q + \frac{\pi}{2} m \pm \frac{\pi}{2} l$ ($l = 0, 1$, and 2) which obviously can be reduced to (6). The system of eight linear equations derived after substitution of (5) and (6) into Eq. (1) was solved numerically to determine $\Omega(q)$. The $\text{Im}[\Omega(q)/\omega]$ curves for the Φ_1 solution are shown in Fig. 3(a). One can see that for any q $\text{Im}[\Omega(q)/\omega] < 0$ at $E_0 = 8000$ is the evidence for stability of the Φ_1 pattern. At $E_0 = 7750$ and $E_0 = 8250$, the Φ_1 pattern is unstable.

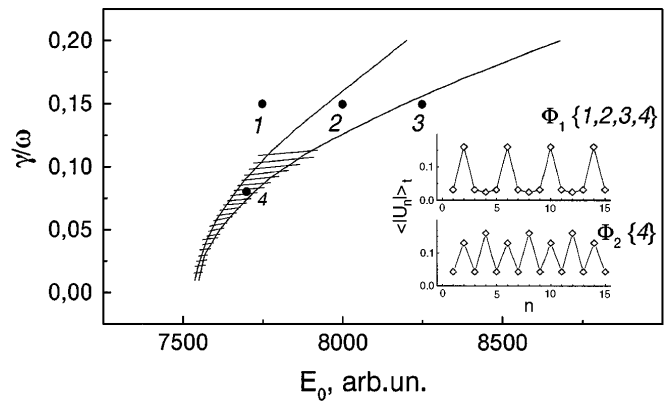


FIG. 2. Boundary curves restricting the Φ_1 pattern stability region in the (γ, E_0) space. In the stretched region there are both stable Φ_1 and unstable Φ_2 patterns. Typical shapes of the Φ_1 and Φ_2 patterns are shown in the inset. Numbers denote the points at which the calculated $\text{Im}[\Omega(q)/\omega]$ are presented in Fig. 3.

$$\begin{aligned} U_n(t) = \frac{1}{2} [V_{C1} \exp(i\omega t + i\varphi_1) \\ + V_{C2} \cos(\frac{\pi}{2} n) \exp(i\omega t + i\varphi_2) \\ + V_{C3} \cos(\pi n) \exp(i\omega t + i\varphi_3) + \text{c.c.}], \end{aligned} \quad (5)$$

where again V_{Cj} are real amplitudes and φ_j are phase angles. According to $\omega = 1.05\omega_0$ and γ values a single stable nontrivial (all $V_{Cj} \neq 0$) solution Φ_1 of the form (5) was found in the region between the solid curves in Fig. 2. Outside this region the solution Φ_1 is unstable in the sense discussed below. An additional and strongly unstable solution Φ_2 exists in the stretched part of the Φ_1 stability region. The time-averaged amplitude $\langle |U_n(t)| \rangle_t$ for the Φ_1 and Φ_2 solutions is presented in the inset in Fig. 2, which shows that both Φ_1 and Φ_2 form coherent dynamical structures (patterns) with symmetry different from that of the external field E . This property has been pointed out recently for a three-particle anharmonic lattice [12]. Note that the Φ_1 pattern can be regarded as a lattice of intrinsic localized vibrations of the odd parity [8,9].

Patterns stability.—For linear stability analysis of the Φ_1 and Φ_2 solutions within RWA, a total perturbation must contain all perturbation waves coupled to each other via four-wave mixing, i.e., all spatial harmonics resulting from a product of any two carrier LSMs from (5) on a perturbation wave. One can see that a set of waves with $k_p = \pm q + \frac{\pi}{2} m$ ($m = 0, 1$, and 2)

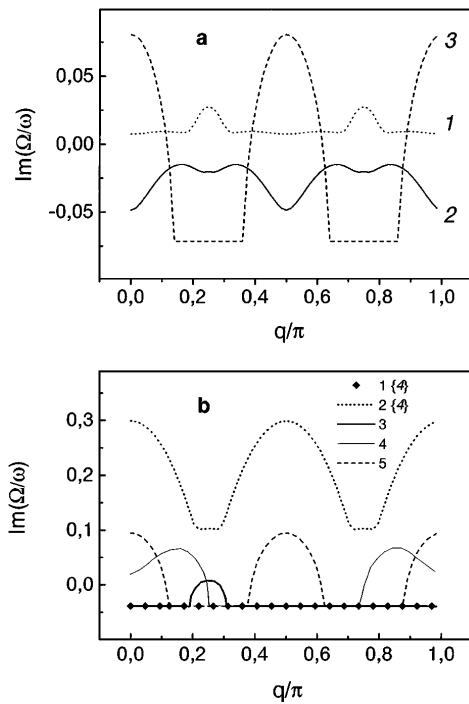


FIG. 3. (a) Relative increment $\text{Im}[\Omega(q)/\omega]$ demonstrating the stability/instability of the Φ_1 pattern for $E_{01} = 7750$, $E_{02} = 8000$, and $E_{03} = 8250$ corresponding to the points 1, 2, and 3, respectively, in Fig. 2; (b) that of the Φ_1 (1 {4}) and Φ_2 (2 {4}) patterns at point 4 in Fig. 2. Curves 3 and 4 show the $\text{Im}[\Omega(q)/\omega]$ for the isolated $k = 0$ and $k = \pi/2$ LSMs forming the Φ_1 pattern at point 4 in Fig. 2. The $k = \pi$ LSM is stable. Curve 5 corresponds to the Φ_1 pattern, but with $\varphi_2 \rightarrow \varphi_2 + \pi/16$.

The increments for the Φ_1 and Φ_2 solutions at point 4 in Fig. 2 are shown by symbols and dotted line, respectively, in Fig. 3(b). One can see the strong instability of the Φ_2 pattern while the Φ_1 pattern is quite stable. The isolated constituent LSMs with $k = 0$ and $k = \pi/2$ of the Φ_1 pattern at point 4 are unstable since $\text{Im}[\Omega(q)/\omega] > 0$ for some q values [curves 3 and 4 in Fig. 3(b)]. One can conclude, therefore, that the Φ_1 pattern stability results from destructive interference of instabilities of the constituent LSMs. Indeed, a small deviation of the phase angle φ_2 on $\pi/16$ from its value leads to the dramatic increase of the increment [curve 5 in Fig. 3(b)].

Figure 4 demonstrates spontaneous pattern formation observed in numerical experiment in the KG lattice. Starting from seeding LSM $V_P = 0.0001 \cos(\frac{\pi}{2} n)$ at $t = 0$, the Φ_1 pattern formation is completed after about 35 periods of external field vibration. The final shape of the particle vibration nearly coincides with that calculated for this case from (1) using (5) (see inset of Fig. 4). In the stretched region in Fig. 2 the unstable solution Φ_2 violates the stable Φ_1 pattern formation and leads to a chaotic behavior of the system. In the case of $N_{\text{LSM}} = 4$ or 5 the stable pattern can be formed starting even from a small-amplitude noise rather than from a seeding wave and can be found in a much broader region of the system parameters than in

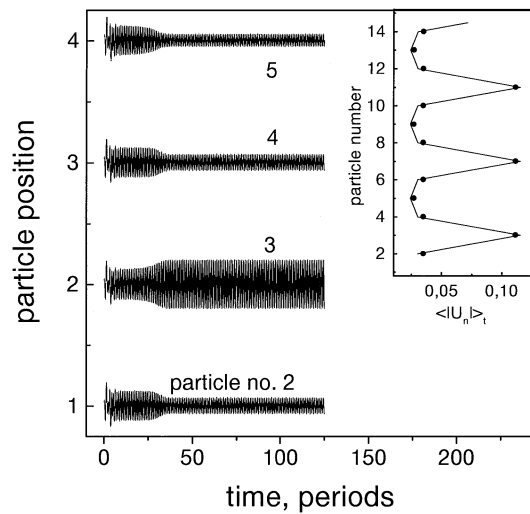


FIG. 4. Particle positions vs time from numerical experiment with the KG lattice with parameters, corresponding to point 2 in Fig. 2, and $q = \pi/2$ seeding LSM. Inset shows the pattern Φ_1 at point 2 in Fig. 2 calculated (solid line) and obtained from numerical experiment (solid circles).

the case of $N_{\text{LSM}} = 3$. An example of the Φ_1 -type pattern observed in the quasi-2D KG lattice with harmonic inter-chain coupling is shown in Fig. 5. The 2D pattern in this case shows periodicity in both parallel and perpendicular to E directions. Detailed study of the 2D patterns will be published elsewhere.

Optical intensity required for the pattern generation.— Our numerical experiments show that to reach the threshold for the pattern formation in our system with $N_{\text{LSM}} = 4$, the particles in the carrier LSM must vibrate with the amplitude $A_p \approx 0.05a$. The electric field strength E_0 of the optical excitation at $\omega = 1.05\omega_0 \approx 10^2 \text{ cm}^{-1}$ can then be estimated using the motion equation in the harmonic approximation. Suggesting $a = 5 \text{ \AA}$ and $\gamma = 0.05\omega_0$, one obtains $E_0 = A_p m_p m_e [(\omega_0^2 - \omega^2)^2 + (\gamma\omega)^2]^{1/2} / (e_p e_e) \approx m_p / e_p [\text{V/cm}]$, where m_p and e_p are the particle mass and the charge measured in the free electron units m_e and e_e , respectively. Accordingly, the field strength is of the order of 1 V/cm for light particles like

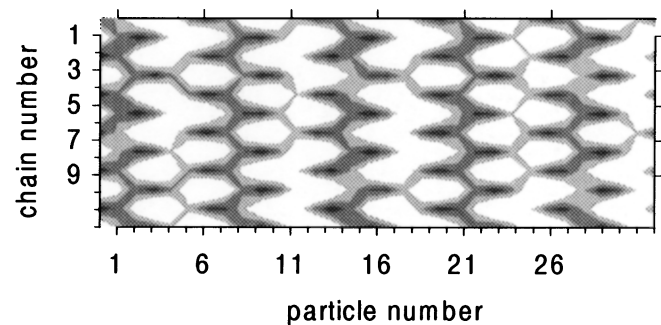


FIG. 5. The $\langle |U_n| \rangle_t$ pattern obtained from numerical experiment with a quasi-2D KG lattice for $\omega \approx 1.05\omega_0$, $\gamma \approx 0.05\omega_0$, and $E_0 = 600$. Nearest neighbor particles in the adjacent chains are coupled via harmonic force constant $K_{\text{int}} = K_2/4$.

electrons and of the order of 10^5 V/cm for ionic solids. The latter value of E_0 can be reached in the laser pulses. Obviously the pulse duration T must be enough for the pattern to be generated and detected. The generation stage lasts over 30–40 periods of vibration, and 10–20 periods are probably needed for the pattern detection in total that means $T \approx 20$ ps. Thus, for the pattern formation in an electronic system (e.g., charge-density wave conductor) the IR laser pulses of energy $W \approx 10^{-11}$ mJ focused into ~ 0.01 cm² are required. The pattern formation in an ionic system needs much higher pulse energy $W \approx 0.1$ mJ, unless the smaller focusing area is used.

The pattern formation under the action of the simple periodic field is, in fact, a way for the ILMs optical generation alternative to that proposed by Rössler and Page and based on use of the suitably controlled sequence of short laser pulses [30]. Although the E_0 values in both methods are very close, the parameters of the generated pattern, which are built of *equal* ILMs, are well defined, in contrast to those of the set of ILMs generated by the short-pulse-sequence method. This fact can be important in experimental detection of the ILMs, which in case of the pattern can be based on effects of dynamical breaking of the lattice translational symmetry.

In conclusion, a first example of the MI mediated pattern formation in the anharmonic lattice is described. The reason for the pattern stability is shown to be closely related to interference of modulation instabilities of constituent spatial modes. Experimental observation of the patterns in a real system would give indirect evidence for existence of intrinsic localized modes.

This work was supported by the Russian Ministry of Science within the program “Fundamental Spectroscopy.”

-
- [1] E. Fermi, J.R. Pasta, and S.M. Ulam, Technical Report No. LA-1940, Los-Alamos Sci., 1955; *Collected Works of E. Fermi* (Chicago Press, Chicago, 1965), Vol. 2, pp. 978–988.
 [2] R.L. Bivins, N. Metropolis, and J.R. Pasta, *J. Comput. Phys.* **12**, 65 (1973).

- [3] N. Saito, N. Niroromi, and A. Ishimura, *J. Phys. Soc. Jpn.* **39**, 1431 (1975).
 [4] M. Toda, *Theory of Nonlinear Lattices* (Springer-Verlag, Berlin, 1981).
 [5] M. Remoissenet, *Phys. Rev. B* **33**, 2386 (1986).
 [6] E.R. Tracy and H.H. Chen, *Phys. Rev. A* **37**, 815 (1988).
 [7] J. Ford, *Phys. Rep.* **213**, 271 (1992).
 [8] A.S. Dolgov, *Sov. Phys. Solid State* **28**, 907 (1986).
 [9] A.J. Sievers and S. Takeno, *Phys. Rev. Lett.* **61**, 970 (1988).
 [10] J.P. Page, *Phys. Rev. B* **41**, 7835 (1990).
 [11] V.M. Burlakov, S.A. Kiselev, and V.N. Pyrkov, *Phys. Rev. B* **42**, 4921 (1990).
 [12] T. Rössler and J.B. Page, *Phys. Rev. B* **51**, 11 382 (1995).
 [13] W.Z. Wang, J.T. Gammel, A.R. Bishop, and M.I. Salkola, *Phys. Rev. Lett.* **76**, 3598 (1996).
 [14] A. Tsurui, *Prog. Theor. Phys.* **48**, 1196 (1972).
 [15] V.M. Burlakov and S.A. Kiselev, *Sov. Phys. JETP* **72**, 854 (1991).
 [16] Y.S. Kivshar and M. Peyrard, *Phys. Rev. A* **46**, 3198 (1992).
 [17] Yuri S. Kivshar, *Phys. Rev. E* **48**, 4132 (1993).
 [18] K.W. Sanduski and J.B. Page, *Phys. Rev. B* **50**, 866 (1994).
 [19] V.M. Burlakov, S.A. Darmanyan, and V.N. Pyrkov, *Sov. Phys. JETP* **108**, 904 (1995).
 [20] V.M. Burlakov, S.A. Darmanyan, and V.N. Pyrkov, *Phys. Rev. B* **54**, 3257 (1996).
 [21] M. Cross and P.C. Hohenberg, *Rev. Mod. Phys.* **65**, 851 (1993).
 [22] F. Melo, P. Umbanhowar, and H.L. Swinney, *Phys. Rev. Lett.* **72**, 172 (1994); **75**, 3838 (1995).
 [23] P. Umbanhowar, F. Melo, and H.L. Swinney, *Nature (London)* **382**, 793 (1996).
 [24] E. Clement *et al.*, *Phys. Rev. E* **53**, 2972 (1996).
 [25] L.S. Tsimring and I.S. Aranson, *Phys. Rev. Lett.* **79**, 213 (1997).
 [26] B. Denardo, W. Wright, S. Putterman, and A. Larraza, *Phys. Rev. Lett.* **64**, 1518 (1990).
 [27] Yuri S. Kivshar, *Phys. Rev. B* **46**, 8652 (1992).
 [28] Yu.S. Kivshar, O.A. Chubukalo, O.V. Usatenko, and D.V. Grinyoff, *Int. J. Mod. Phys. B* **9**, 2963 (1995).
 [29] T. Rössler and J.B. Page, *Phys. Lett. A* **204**, 418 (1995).
 [30] T. Rössler and J.B. Page, *Phys. Rev. Lett.* **78**, 1287 (1997).